Serican Journal of Medicine
2026, VOL. 3, NO. 3, 25651
https://doi.org/10.17161/sjm.v3i3.25651

FOXA2 overexpression induces prostate tumors with mixed adenocarcinoma and neuroendocrine histology

Xiaodong Lu[1], Viriya Keo[1], Hongshun Shi[1], Liu Peng[1], Lara R Harik[3,4], and Jindan Yu[1,2,4]

[1]Department of Urology, Emory University School of Medicine, Atlanta, GA 30322, USA; [2]Department of Human Genetics, Emory University School of Medicine, Atlanta, GA 30322, USA; [3]Department of Pathology and Laboratory Medicine, Emory University School of Medicine, Atlanta, GA 30322, USA; [4]Winship Cancer Institute, Emory University School of Medicine, Atlanta, GA 30322, USA

Correspondent author: Jindan Yu, MD/PhD, Fray Marshall Chair in Biomedical Urology Research, Professor and Vice Chair for Research in the Department of Urology, Emory University School of Medicine, Health Sciences Research Building (HSRB1) Third Floor, E330, 1760 Haygood Dr NE, Atlanta, GA 30322.
Phone: 404-778-6871; E-mail: jindan.yu@emory.edu

ABSTRACT

Following prolonged androgen receptor (AR)-targeted therapy, approximately 20% of castration-resistant prostate cancers (CRPC) progress to AR-independent subtypes. This includes neuroendocrine prostate cancer (NEPC), a highly aggressive variant with dismal clinical outcomes and limited treatment options. The pioneer transcription factor FOXA2 has been shown to drive this neuroendocrine trans-differentiation (NET), yet the precise histological characteristics of FOXA2-driven tumors remain poorly defined. In this study, we demonstrate that FOXA2 overexpression in both xenograft and allograft prostate cancer models gives rise to tumors with mixed histologic features, resembling treatment-induced NEPC in patients. Notably, FOXA2-expressing tumors developed distinct NEPC foci characterized by poorly differentiated histopathology, neuroendocrine gene expression, and significantly elevated Ki-67 proliferation indices within predominantly adenocarcinoma tumors, indicating cellular heterogeneity in FOXA2 expression, lineage plasticity, and differential responses to local microenvironmental cues in vivo. Together, these findings validate FOXA2 as a master regulator of lineage plasticity and NEPC transformation in vivo and underscore the clinical relevance of FOXA2 overexpression models in studying NEPC transformation.

ARTICLE HISTORY
Received: June 19, 2026
Revised: July 14, 2026
Accepted: July 14, 2026

KEYWORDS
FOXA2, heterogeneous tumors, neuroendocrine transdifferentiation, mixed histology

1. Introduction

Prostate cancer is the most diagnosed cancer in American men. Most prostate cancers are initially diagnosed as adenocarcinomas and are highly dependent on androgens. Androgen deprivation therapy (ADT) is the mainstay treatment for prostate cancer (PCa). While most PCa originally responds well to ADT, the tumors eventually recur and progress to castration-resistant prostate cancer (CRPC). Further treatment with second-generation androgen receptor (AR) pathway inhibitors, such as enzalutamide and abiraterone, can extend survival, but as high as 20% of CRPC cases may progress into AR-independent prostate cancers, including neuroendocrine prostate cancer (NEPC) and double-negative prostate cancer (DNPC) [1-3].

NEPC is characterized by the loss of AR signaling pathway gene expression and the gain of neuroendocrine lineage marker genes. In contrast, DNPC exhibits low expression of both AR target genes and neuroendocrine genes [4]. Recent studies suggest that DNPC may acquire some squamous differentiation features [5]. These AR-independent cancers are highly aggressive, with a median survival of less than one year. Given the poor prognosis, a DNPC or NEPC model that accurately recapitulates human PCa transformation is urgently needed. Such a model would be essential for elucidating the molecular mechanisms underlying this aggressive disease and for identifying key molecular targets for therapeutic intervention.

CRPC and NEPC share many genetic alterations, with *RB1* deletion and *p53* mutation being more enriched in NEPC. Several genetically engineered mouse models (GEMMs), such as $Pten^{f/f}$;$Rb1^{f/f}$ (PR), $Pten^{f/f}$;$p53^{f/f}$ (PP), $Pten^{f/f}$;$Rb1^{f/f}$;*Mycn*+ (PRN), and

Pten$^{f/f}$;p53$^{f/f}$;Rb1$^{f/f}$ (PPR) mice with prostate-specific deletion or overexpression of indicated genes, have been created to study CRPC progression to NEPC [6-9]. These models initially develop high-grade adenocarcinoma and subsequently evolve into heterogeneous tumors exhibiting divergent differentiation. Depending on the model, tumors may retain a conventional adenocarcinoma phenotype or acquire neuroendocrine, squamous, and/or sarcomatoid features. Notably, the PRN and PPR models display more aggressive and poorly differentiated tumors compared to the PP and PR models, underscoring the synergistic role of *RB1* loss, *p53* mutation, and *Mycn* amplification in driving NEPC aggressiveness.

FOXA2 is a pioneer transcription factor that is highly expressed in NEPC and serves as a diagnostic marker for this aggressive subtype [10-12]. Genetic studies in mice have established that Foxa2 is essential for NEPC transformation, mediating its effects through the KIT and hypoxia pathways [13, 14]. Our recent work demonstrated that FOXA2 overexpression in prostate adenocarcinoma cell lines induces NEPC trans-differentiation by remodeling both 2D and 3D chromatin architecture [15]. However, a comprehensive histopathological characterization of FOXA2-driven NEPC tumors is still lacking.

In this study, we demonstrate that Foxa2 promotes NEPC transformation across multiple preclinical models, including the PP mouse PCa organoids and allografts, as well as LNCaP xenografts. FOXA2 induced heterogeneous tumors with a mixed histology, including adenocarcinoma and neuroendocrine tumors. Notably, tumor foci with NE features exhibited significantly elevated expression of the proliferation marker Ki-67 and displayed poorly differentiated histology compared to adenocarcinoma foci. These findings underscore the clinical relevance of FOXA2 overexpression models in studying NEPC transformation.

Materials and methods

Ethics statement

Our research complies with all relevant ethical regulations. Mouse handling and experimental procedures were approved by the Institutional Animal Care and Use Committee at Northwestern University in accordance with the US National Institutes of Health Guidelines for the Care and Use of Laboratory Animals and the Animal Welfare Act.

3D organoid cell culture

Mouse prostate organoids were generated as previously described[16]. Briefly, prostates from 7- to 8-week-old *PbCre$^{-/-}$*; *Pten$^{f/f}$*; *p53$^{f/f}$* mice were minced into small pieces (~1 mm^3) and digested in 5 mg/mL collagenase type II (Gibco, #17101-015) supplemented with 10 μM Y-27632 dihydrochloride (Tocris, #1254) for 1–1.5 h at 37°C. The digested tissue was washed once with Advanced DMEM/F12 (adDMEM/F12) containing penicillin/streptomycin, 10 mM HEPES, and 2 mM GlutaMAX (adDMEM/F12 +/+/+), then resuspended in 5 mL TrypLE Express (Gibco, #12604-021) for further digestion at 37°C for 15 min. After digestion, cells were washed once with adDMEM/F12 +/+/+, counted using a hemocytometer, and 20,000 cells were plated in a 40 μL Matrigel drop in the center well of a 12-well plate. The plate was incubated (5% CO_2, 37°C) for 15 min to allow Matrigel polymerization. Subsequently, 1 mL of prewarmed mouse complete organoid medium supplemented with 10 μM Y-27632 was gently added, and cultures were maintained in a CO_2 incubator (5% CO_2, 37°C). Medium was refreshed every 3 days. For passaging, organoids were collected weekly at a 1:4 split ratio. Matrigel and organoids were washed with PBS, resuspended in 0.5 mL TrypLE Express, and digested at 37°C for 15 min. After digestion, cells were washed once with adDMEM/F12 +/+/+ and replated in 50% Matrigel before adding fresh organoid culture medium.

Lentiviral infection of mouse organoids

For lentiviral infection, dissociated single cells were mixed with lentivirus in the presence of 8 μg/mL polybrene and centrifuged at 600 × g for 1 h at room temperature. After centrifugation, cells were incubated at 37°C with 5% CO_2 for 6 h to allow viral uptake, then embedded in Matrigel for further culture.

Murine xenograft and allograft studies

Mice were housed in specific pathogen-free animal facilities (at 20–23 °C, with 40–60% humidity and 12-h light/12-h dark cycle). NOD SCID male mice at 6–7 weeks old were purchased from Charles River Laboratories. For LNCaP/plv and LNCaP/FOXA2 xenografts, 2x10^6 cells were subcutaneously injected into the right flank of the mice. Tumor volumes were measured twice weekly using digital calipers and calculated as: $V = L \times W^2/2$ (V, mm3; L, mm; W, mm).

For the allograft study, control- or Foxa2-expressing prostate organoids from PbCre-negative Pten and p53 knockout mice were infected with Cre virus *in vitro* and then amplified in Matrigel for one week. Subsequently, 2 million dissociated organoids were injected subcutaneously into the flanks of SCID mice. The tumor growth was monitored as described above.

Western blotting and Immunohistochemistry (IHC)

Western blotting was performed using established protocols and antibodies (**Supplementary Table 1**). IHC was performed using ImmPRESS® Excel Amplified Polymer Kit (Vector Laboratories), according to the manufacturer's instructions. Briefly, Formalin-fixed paraffin-embedded (FFPE) tissue sections were de-paraffinized and hydrated, followed by antigen retrieval, which was accomplished by heating at 99–100 °C for 15 min in 1x citrate buffer, pH 6.0 (Sigma, C9999-1000ML). Following antigen retrieval, the tissue sections were incubated with BLOXALL blocking solution to quench endogenous peroxidase activity and then were blocked with 2.5% normal horse serum. After blocking, the tissue sections were incubated with primary antibodies (AR, cat#ab108341, 1:1000; FOXA2, cat#ab108422, 1:1000; SYP, cat#sc-17750, 1:100; Ki67, cat#ab16667, 1:150) followed by incubating with amplifier antibody (Goat Anti-Rabbit IgG for rabbit primary antibodies) or directly incubated with ImmPRESS polymer reagent (for mouse primary antibodies). After ImmPRESS polymer reagent incubation, the tissue sections were incubated in ImmPACT DAB EqV working solution until desired stain intensity developed, then the tissue sections were counterstained with hematoxylin, mounted with mounting medium, and imaged with an Olympus microscope. All histological evaluations and quantifications (including hematoxylin and eosin (H&E)-stained and IHC images) were performed by a board-certified, genitourinary pathologist (L.H.) who was blinded to animal genotypes.

Bulk RNA-Seq Analysis

Raw counts of genes were calculated by STAR. Fragments per kilobase of transcript per million mapped reads (FPKM) values were calculated by an in-house Perl script. Differential gene expression analysis was performed using DESeq2 with default parameters. Pathway enrichment analysis was performed using GSEA.

Statistical analysis

For each independent *in vitro* experiment, at least three technical replicates were used. Most *in vitro* experiments were repeated independently three times, and some were repeated twice. Two-tailed unpaired Student's *t*-tests were used to assess statistical significance in RT-qPCR experiments and cell-based functional assays and *in vivo* mouse experiments.

Results

Foxa2 induces neuroendocrine differentiation of mouse PCa organoids with Pten and p53 double knockout

To investigate whether Foxa2 can induce neuroendocrine differentiation of mouse PCa, we generated organoid cultures of prostate cancer tissues derived from the *Pbcre*$^{-/-}$;*Pten*$^{f/f}$;*p53*$^{f/f}$ (PP) mouse and infected them with either Cre lentivirus alone or Cre combined with Foxa2 lentivirus (**Fig.1A**). Western blot analysis confirmed double knockout (DKO) of both *pten* and *p53* upon Cre lentivirus infection. Notably, androgen receptor (AR) expression was significantly downregulated in organoids with Foxa2 overexpression (OE) (**Fig. 1B**), suggesting that Foxa2 may promote lineage plasticity. To further validate this, we assessed the expression of Ar and neuroendocrine (NE) marker genes in control and Foxa2-OE organoids. Foxa2 markedly induced the expression of NE markers, including Syp, Chga, Ncam1, and Insm1, at RNA and/or protein levels (**Fig. 1C**). Together, these findings demonstrate that Foxa2 drives neuroendocrine differentiation of PP-DKO mouse prostate cancer organoids.

Foxa2 induces luminal-to-neuronal transcriptional reprogramming in PP mouse PCa organoids

To investigate the transcriptional programs regulated by Foxa2, we performed RNA sequencing (RNA-seq) in control and Foxa2-OE PP mouse PCa organoids and identified differentially expressed genes. Notably, genes upregulated in Foxa2-OE cells were enriched for pathways associated with cell motility, neurogenesis, and epithelial cell differentiation, while downregulated genes were involved in luminal epithelial cell functions, such as cell adhesion and response to stimulus (**Fig. 2A**). We noticed that cell differentiation programs were enriched by both gene sets. A close look revealed that they involve distinct genes (**Supplementary Table 1**). Genes upregulated

Figure 1. Foxa2 overexpression in PP-DKO (double-knockout) prostate organoids induces neuroendocrine differentiation

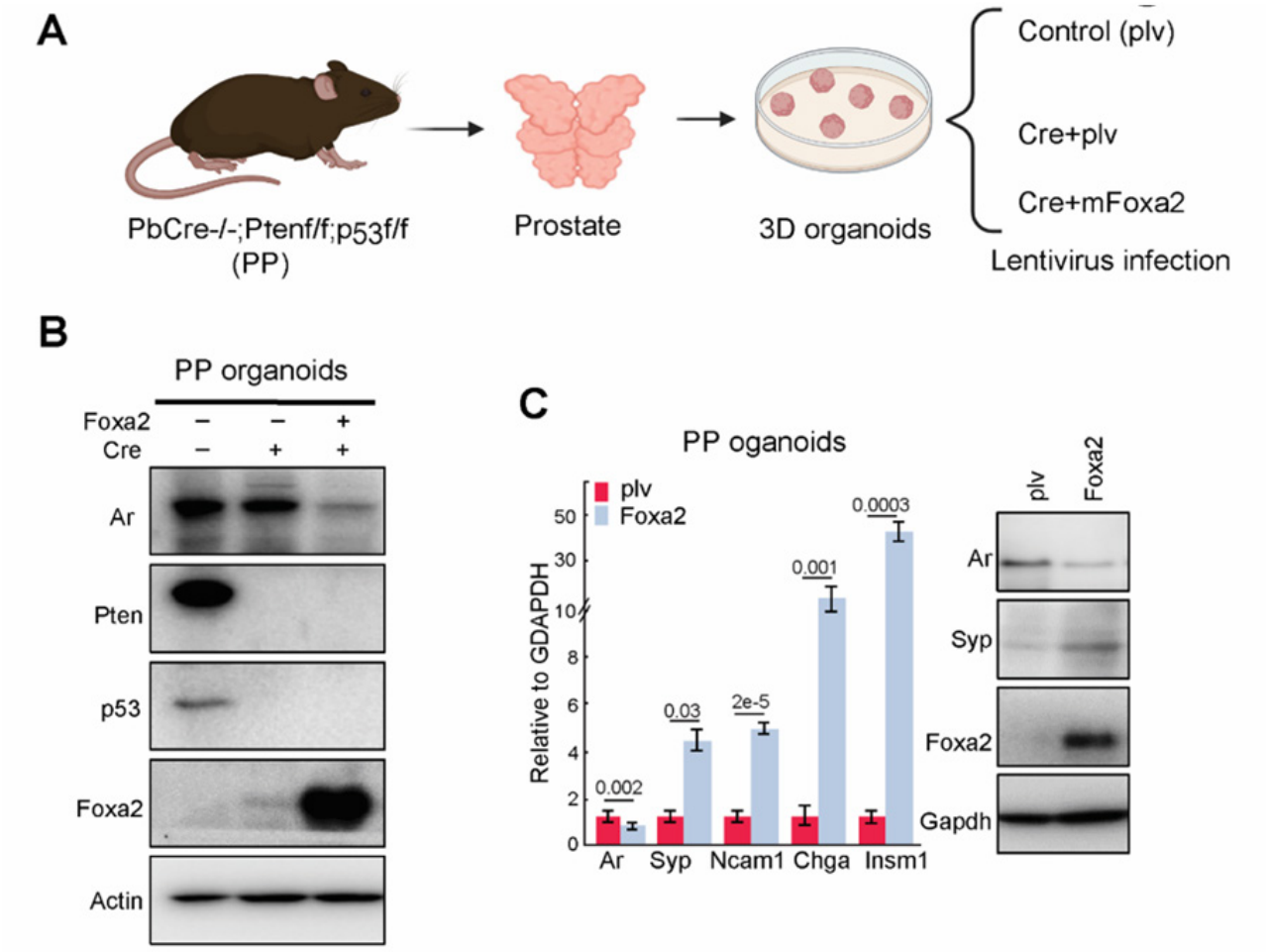

A. Schema illustrating the generation of control (plv) and Foxa2-overexpressing (Foxa2-OE) organoids from PP mice.

B. Western blot (WB) confirming knockout of Pten and p53, and overexpression of Foxa2 in the PP organoids with indicated treatment.

C. RT-PCR (left) and WB (right) showing that Foxa2 OE induced NE marker gene expression. Data were normalized to *GAPDH* (mean ± SEM, n =3). *P* values were calculated by an unpaired two-sided *t*-test.

in Foxa2 OE cells were enriched for molecular pathways involved in epithelial cell differentiation and exhibited a distinct neuroendocrine (NE) signature, characterized by the induction of key regulators such as Ascl1, Insm1, Bmp4, and Lef1 (**Fig. 2B and Supplementary Table 1**). Conversely, the downregulated genes are predominantly involved in extracellular matrix remodeling and epithelial-mesenchymal transition, as evidenced by the repression of structural and signaling markers including Col5a1, Mmp9, Tgfb3, Sfrp1, and Cd34 (**Supplementary Table 1**). Taken together, these findings demonstrate that Foxa2 promotes neuronal transcriptional programs in the mouse PP PCa organoids, while repressing luminal phenotypes.

Foxa2 drives androgen-independent PCa growth

Given the downregulation of Ar in Foxa2-OE organoids, we investigated whether Foxa2 drives androgen-independent growth. We cultured control and Foxa2-OE organoids in both androgen-supplemented and androgen-depleted medium. Under androgen-supplemented conditions, while the size of Foxa2-OE organoids remained comparable to controls, their number was significantly increased (**Fig. 3A**). Importantly, under androgen-depleted conditions, control organoids exhibited markedly reduced growth compared to androgen-supplemented conditions, but Foxa2-OE organoids maintained robust proliferation (**Fig. 3B**). These findings suggest that Foxa2 OE robustly drives androgen-independent PCa growth.

Figure 2. Foxa2 overexpression in PP-DKO prostate organoids induces neuronal transcriptional signatures.

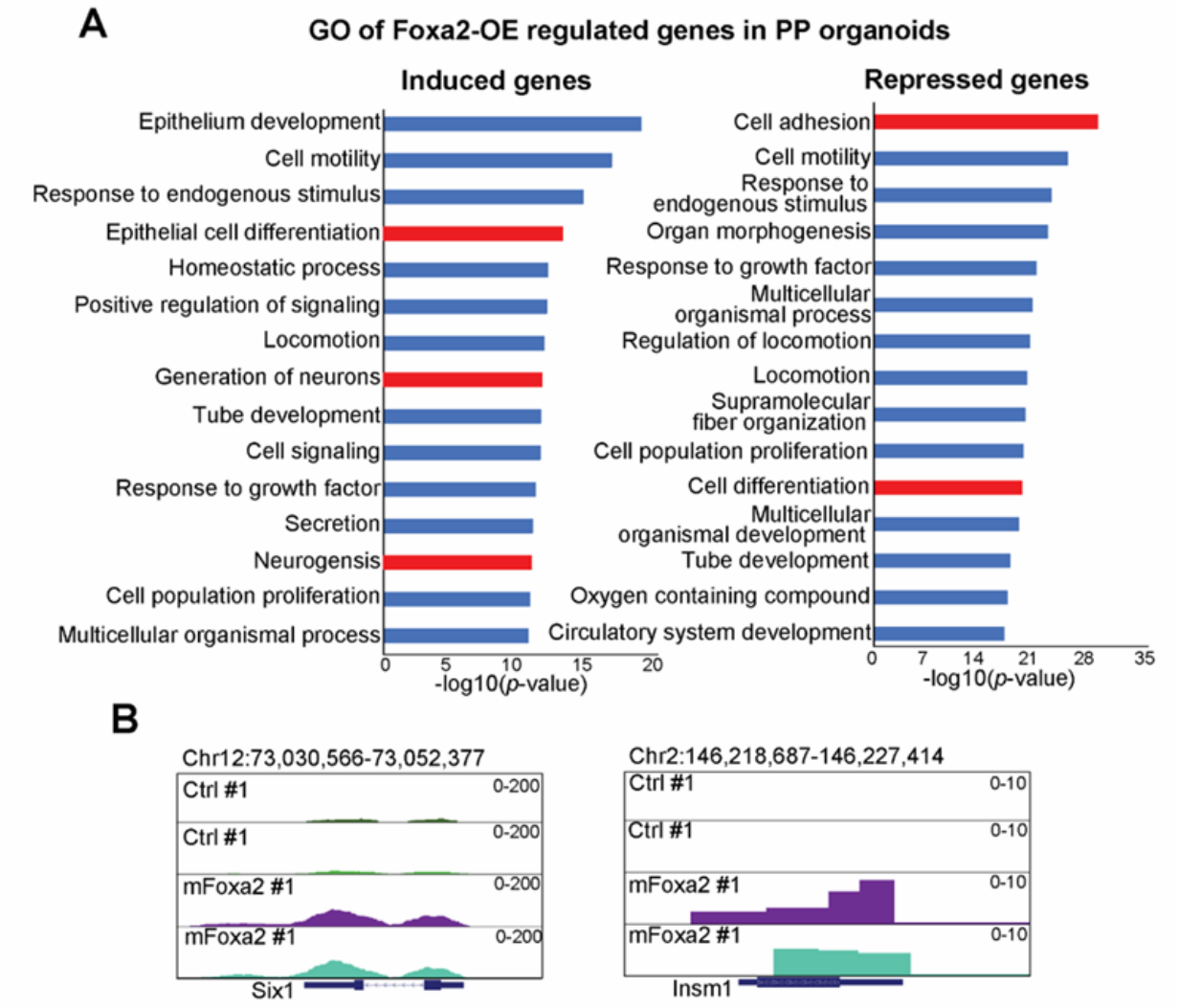

A. Gene set enrichment analysis of Foxa2-induced and -repressed genes in PP organoids. The most enriched molecular concepts are shown on the Y-axis, while the X-axis indicates enrichment significance. Neuron and cell differentiation-related GO terms are highlighted in Red. **B**. Genome browser views showing that the mRNA levels of neuronal lineage genes *Six1* and *Insm1* were increased in Foxa2-OE organoids compared to controls.

Figure 3. Foxa2 overexpression promotes androgen-dependent and androgen-independent PP-DKO PCa organoid growth

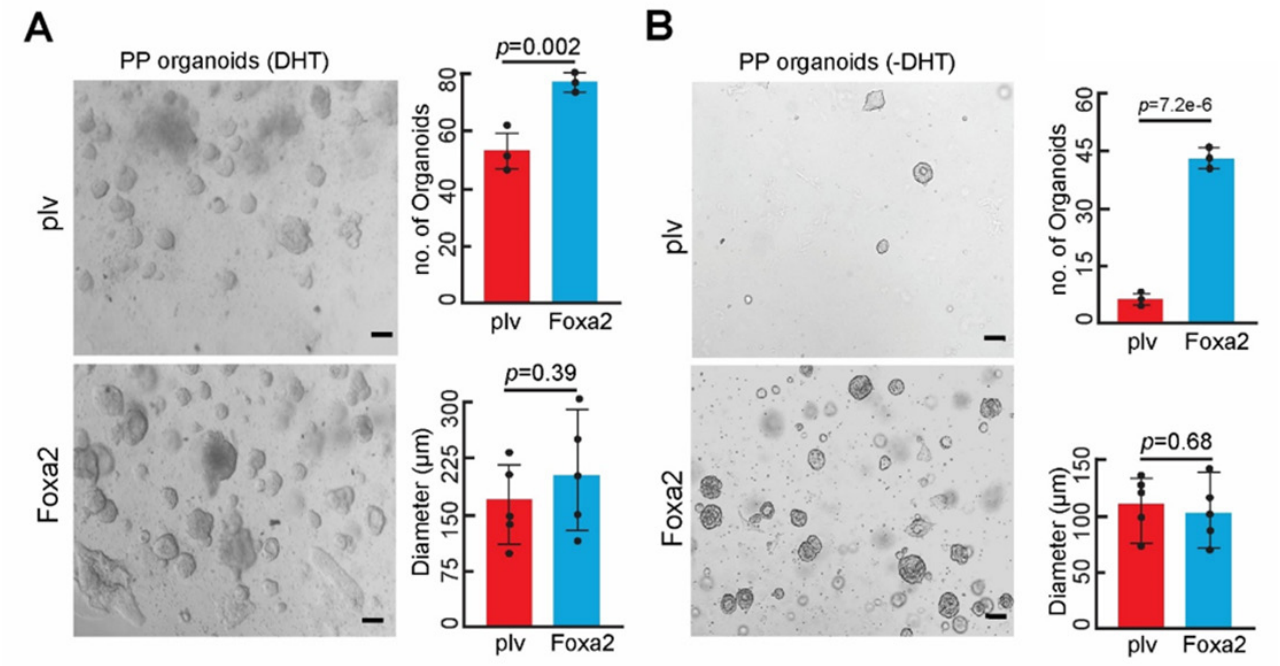

A-B. Representative brightfield images showing the morphology of control and Foxa2-OE organoids maintained in androgen (A, DHT, 1nM) and androgen-depleted (B) conditions. The number and diameter of organoids are quantified on the right.

Foxa2-OE PP PCa organoids grow allograft prostate tumors with a mixed histology

Given that Foxa2 OE enhances organoid growth in vitro, we next examined its specificity in driving NEPC *in vivo*. Control and Foxa2-OE organoids were inoculated into the flanks of NOD/SCID mice. We observed notable differences in tumor growth between control and Foxa2-OE groups as early as 2 weeks post-inoculation, which showed a more pronounced difference by week 6 (**Fig. 4A**). Consistent with this, endpoint tumors in Foxa2-OE mice were substantially larger than those in the control mice (**Fig. 4B**), confirming that Foxa2 drives PP-DKO allograft tumor growth.

Histopathological analysis revealed that most tumors in both groups exhibited adenocarcinoma features (81.7% control vs. 74.2% Foxa2-OE cells), with a minor subset (~6% in both groups) showing squamous differentiation (**Fig. 4C**), a pattern that is consistent with prior observations in *Pten*$^{f/f}$;*p53*$^{f/f}$ and *Pten*$^{f/f}$;*Rb1*$^{f/f}$;*Mycn*$^{+}$ GEMM models [9]. Notably, control tumors occasionally displayed sarcomatoid differentiation, which was also previously reported in the *Pten*$^{f/f}$;*p53*$^{f/f}$ model [9]. Strikingly, Foxa2-OE tumors exhibited a significant increase in tumor cells with neuroendocrine (NE) differentiation (19.6% vs. 0% in controls) (**Fig. 4C**), indicated by condensed nuclei and scant cytoplasm. Immunohistochemistry (IHC) demonstrated a global loss of the luminal marker Ar in Foxa2-OE tumors, in both adenocarcinoma and poorly differentiated NE phenotypes (**Fig. 4D**). By contrast, the NE marker synaptophysin (Syp) was selectively elevated in poorly differentiated regions with NE morphology, in contrast to its undetectable expression in adenocarcinomas. Critically, NE-differentiated regions also showed markedly higher staining of the proliferation marker Ki-67 than adenocarcinoma regions (**Fig. 4D**). Taken together, these findings demonstrate that FOXA2 overexpression broadly inhibits luminal gene expression, while only a small fraction of cells fully acquire a neuroendocrine phenotype, mirroring the mixed histology of treatment-induced NEPC in patients.

FOXA2-OE LNCaP cells grow xenograft tumors with a mixed histology

To further investigate the extent of FOXA2 in promoting NE differentiation in human PCa, we established LNCaP xenografts with either control or FOXA2-OE cells. We have previously shown that FOXA2-OE LNCaP cells grow xenograft tumors at a considerably faster speed than the control cells [15].

Figure 4. Foxa2-OE PP PCa organoids grow allograft prostate tumors with a mixed histology

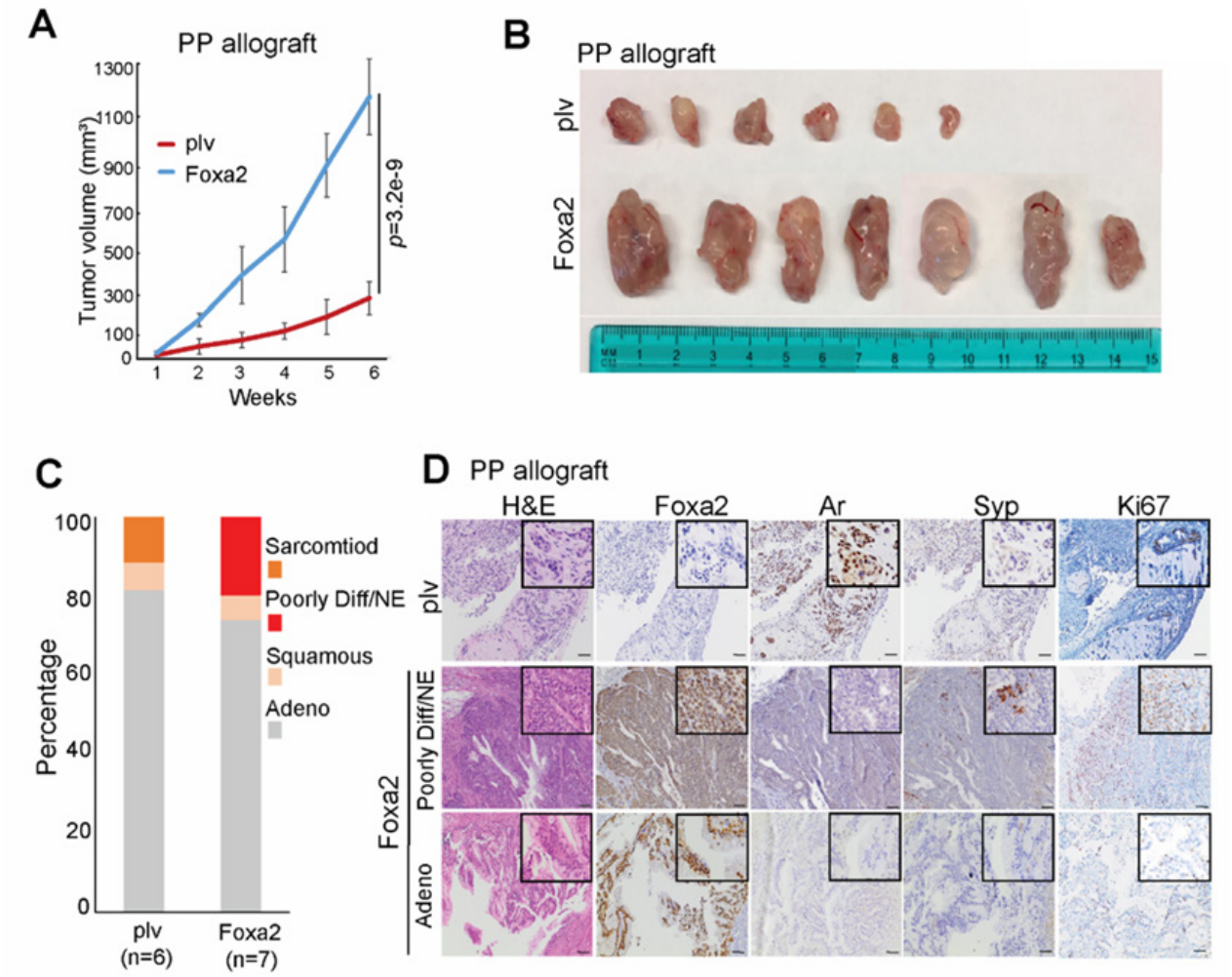

A-B. Foxa2 OE promotes *Pten*$^{f/f}$;*p53*$^{f/f}$ (PP) allograft tumor growth. (A) Tumor growth curves of control and Foxa2-overexpressing (Foxa2-OE) allografts. (B) Representative tumor images from each group at endpoint.

C. Quantification of tumor histology based on pathologist assessment. Shown is the percentage of tumor foci exhibiting conventional adenocarcinoma (including HGPIN and adenocarcinoma), poorly differentiated/neuroendocrine (Poorly Diff/NE) features, squamous differentiation, or sarcomatoid differentiation in control and Foxa2-OE groups.

D. Representative H&E (left) and immunohistochemistry (IHC, right) images of tumor foci. Control tumors primarily exhibit adenocarcinoma (Adeno) morphology, whereas Foxa2-OE tumors display mixed features of Adeno and Poorly Diff/NE differentiation. IHC staining for Ar (adenocarcinoma marker), Syp (neuroendocrine marker), and Ki-67 (proliferation marker). Scale bar, 30 μm. Insets show higher-magnification views.

Histopathological examination revealed markedly different tumor morphology, with FOXA2-OE cells exhibiting features indicative of a much higher grade and poor differentiation (**Fig. 5A**). Moreover, all control tumors exhibited an adenocarcinoma phenotype, whereas FOXA2-overexpressing tumors consisted predominantly of adenocarcinoma (~95%) with a minor component of classical neuroendocrine differentiation (~5%), as we have previously reported [15].

At the molecular level, IHC analysis demonstrated that control LNCaP xenograft tumors, as expected, expressed high levels of AR but did not express FOXA2 and the NE marker SYP. In contrast, FOXA2-OE tumors exhibited a loss of AR expression and a huge increase in FOXA2, SYP, and Ki67 levels in both adenocarcinoma and NE-differentiated foci, with the latter showing much stronger staining intensities for all three (**Fig. 5B**). This data confirms that FOXA2

Figure 5. FOXA2 overexpression drives LNCaP xenograft tumors with a mixed histology

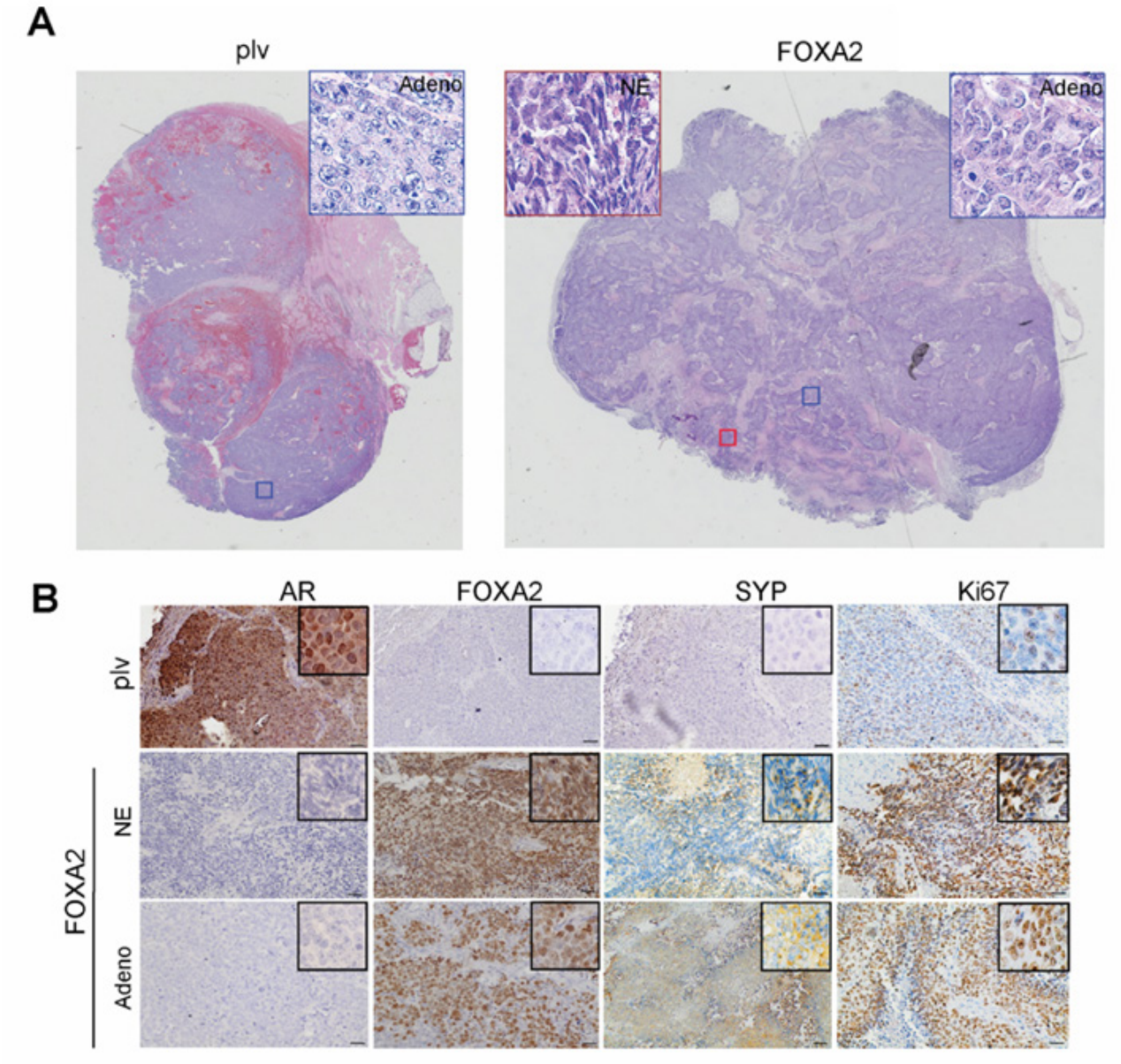

A. Representative H&E images (4× magnification) of tumor foci. Control (plv) tumors display conventional adenocarcinoma (Adeno) morphology (left). FOXA2-OE tumors exhibit mixed histology with regions of Adeno (blue square) and neuroendocrine (NE) differentiation (red square). Scale bar, 30 μm. Insets show higher magnification of boxed regions.

B. Representative immunohistochemistry (IHC) images of tumor foci. Control tumors exhibit adenocarcinoma features, while FOXA2-OE tumors contain both Adeno and NE components. IHC markers: AR (adenocarcinoma), SYP (neuroendocrine), and Ki-67 (proliferation). Scale bar, 30 μm. Insets show higher-magnification views.

OE leads to tumors with a mixed histology of adenocarcinoma and NEPC, similar to allograft mouse PP PCa and clinical treatment-induced NEPC.

Discussion

NEPC is an aggressive variant of prostate cancer, and developing models that faithfully recapitulate clinical NEPC transformation is critical for understanding its biology and identifying therapeutic targets. In this study, we demonstrated that Foxa2 OE induces luminal-to-neuronal transcriptional reprogramming, promotes PCa cell growth, and promotes androgen-independent growth in the PP mouse PCa organoid model. Moreover, Foxa2 drove the forma-

tion of mixed adenocarcinoma (most) and neuroendocrine tumors (less) in both allograft and xenograft models, suggesting that FOXA2-induced tumors are heterogeneous and the AR-/NE- tumors may be a transient state between adenocarcinoma and neuroendocrine cancer. The features were consistent with observations in *Pten*$^{f/f}$;*p53*$^{f/f}$ and *Pten*$^{f/f}$;*Rb1*$^{f/f}$;*Mycn*+ models, where some adenocarcinomas also lack both AR and NE marker gene expression.

Interestingly, not all FOXA2-expressing tumor foci exhibited neuroendocrine features, despite comparable FOXA2 expression and reduced AR levels in both adenocarcinoma and NEPC regions. These findings contrast with our in vitro observations, in which FOXA2 OE induced a complete luminal-to-neuroendocrine lineage transition by 28 days post-induction. This discrepancy may be attributable to several factors. First, the duration of FOXA2 expression in mice might have been insufficient to support complete lineage conversion for all cells, consistent with observations from the PRCAB model [17, 18], where tumors predominantly exhibit adenocarcinoma features at early time points. Second, the enrichment of FOXA2-expressing cells may have been less complete in vivo than in vivo, because antibiotic selection could not be applied, resulting in heterogeneous and potentially lower levels of FOXA2 expression across tumor cells. Third, as we have shown in our recent publication [19], even during a complete NET in vitro, some FOXA2-overexpressing cells remain luminal, alongside a larger proportion of NE cells, as determined by scRNA-seq and scATAC-seq. Individual cells could exhibit varying levels of FOXA2 overexpression and degrees of lineage plasticity, thus growing tumors of different histology. Lastly, FOXA2-driven neuroendocrine transformation might be affected by additional cues *in vivo*, such as hormonal and tumor immune microenvironment. This latter possibility aligns with the clinical observation that treatment-induced NEPC frequently exhibits mixed histology, with neuroendocrine and adenocarcinoma components coexisting within the same tumor. Furthermore, consistent with clinical NEPC, which is characterized by highly aggressive behavior, elevated proliferative indices, and histological features including nuclear condensation and scant cytoplasm, NEPC foci in both models used in this study exhibited similar morphology and significantly higher Ki-67 expression than adenocarcinoma regions. These findings further support the relevance of the FOXA2-overexpression models for studying NEPC transformation.

Acknowledgements

This work was partially supported by the Northwestern University Pathology Core Facility, Emory University Pathology Core Facility, and Emory Imaging Core Facility. NGS was done at the University of Chicago Genomics Facility. We thank members of the Yu lab for helpful discussions. Funding support for the work includes the Prostate Cancer SPORE P50CA180995 (JY, XY), R01CA257446 (JY), 1R01CA286147 (JCZ, JY), Department of Defense PC210266 (JY), and Prostate Cancer Foundation 2017CHAL2008 (JY, JCZ).

Contributions: J.Y. and X.L. conceived the project and designed the experiments. V.K., X.L., and J.Y. conducted bioinformatic and statistical analyses. X.L. and L.H. performed IHC and H&E evaluations and quantifications. X.L., H.S., and L.P. performed all other experiments. X.L. and J.Y. wrote the manuscript. All authors approved the manuscript.

Conflict of Interest: All authors have declared that no conflict of interest exists.

References

1. Beltran H, Prandi D, Mosquera JM, Benelli M, Puca L, Cyrta J, Marotz C, Giannopoulou E, Chakravarthi BV, Varambally S *et al*: **Divergent clonal evolution of castration-resistant neuroendocrine prostate cancer**. *Nat Med* 2016, **22**(3):298–305. doi:10.1038/nm.4045: PMC4777652.
2. Aggarwal R, Huang J, Alumkal JJ, Zhang L, Feng FY, Thomas GV, Weinstein AS, Friedl V, Zhang C, Witte ON *et al*: **Clinical and Genomic Characterization of Treatment-Emergent Small-Cell Neuroendocrine Prostate Cancer: A Multi-institutional Prospective Study**. *J Clin Oncol* 2018, **36**(24):2492–2503. doi:10.1200/JCO.2017.77.6880: PMC6366813.
3. Bluemn EG, Coleman IM, Lucas JM, Coleman RT, Hernandez-Lopez S, Tharakan R, Bianchi-Frias D, Dumpit RF, Kaipainen A, Corella AN *et al*: **Androgen Receptor Pathway-Independent Prostate Cancer Is Sustained through FGF Signaling**. *Cancer Cell* 2017, **32**(4):474–489 e476. doi:10.1016/j.ccell.2017.09.003: PMC5750052.

4. Beltran H, Hruszkewycz A, Scher HI, Hildesheim J, Isaacs J, Yu EY, Kelly K, Lin D, Dicker A, Arnold J *et al*: **The Role of Lineage Plasticity in Prostate Cancer Therapy Resistance**. *Clin Cancer Res* 2019, **25**(23):6916–6924. doi:10.1158/1078-0432. CCR-19-1423: PMC6891154.
5. Labrecque MP, Coleman IM, Brown LG, True LD, Kollath L, Lakely B, Nguyen HM, Yang YC, da Costa RMG, Kaipainen A *et al*: **Molecular profiling stratifies diverse phenotypes of treatment-refractory metastatic castration-resistant prostate cancer**. *J Clin Invest* 2019, **129**(10):4492–4505. doi:10.1172/JCI128212: PMC6763249.
6. Ku SY, Rosario S, Wang Y, Mu P, Seshadri M, Goodrich ZW, Goodrich MM, Labbe DP, Gomez EC, Wang J *et al*: **Rb1 and Trp53 cooperate to suppress prostate cancer lineage plasticity, metastasis, and antiandrogen resistance**. *Science* 2017, **355**(6320):78–83. doi:10.1126/science.aah4199: PMC5367887.
7. Tan HL, Sood A, Rahimi HA, Wang W, Gupta N, Hicks J, Mosier S, Gocke CD, Epstein JI, Netto GJ *et al*: **Rb loss is characteristic of prostatic small cell neuroendocrine carcinoma**. *Clin Cancer Res* 2014, **20**(4):890–903. doi:10.1158/1078-0432. CCR-13-1982: PMC3931005.
8. Dardenne E, Beltran H, Benelli M, Gayvert K, Berger A, Puca L, Cyrta J, Sboner A, Noorzad Z, MacDonald T *et al*: **N-Myc Induces an EZH2-Mediated Transcriptional Program Driving Neuroendocrine Prostate Cancer**. *Cancer Cell* 2016, **30**(4):563–577. doi:10.1016/j.ccell.2016.09.005: PMC5540451.
9. Zou M, Toivanen R, Mitrofanova A, Floch N, Hayati S, Sun Y, Le Magnen C, Chester D, Mostaghel EA, Califano A *et al*: **Transdifferentiation as a Mechanism of Treatment Resistance in a Mouse Model of Castration-Resistant Prostate Cancer**. *Cancer Discov* 2017, **7**(7):736–749. doi:10.1158/2159-8290.CD-16-1174: PMC5501744.
10. Park JW, Lee JK, Witte ON, Huang J: **FOXA2 is a sensitive and specific marker for small cell neuroendocrine carcinoma of the prostate**. *Mod Pathol* 2017, **30**(9):1262–1272. doi:10.1038/modpathol.2017.44: PMC6330177.
11. Mirosevich J, Gao N, Gupta A, Shappell SB, Jove R, Matusik RJ: **Expression and role of Foxa proteins in prostate cancer**. *Prostate* 2006, **66**(10):1013–1028. doi:10.1002/pros.20299:
12. Wang Z, Townley SL, Zhang S, Liu M, Li M, Labaf M, Patalano S, Venkataramani K, Siegfried KR, Macoska JA *et al*: **FOXA2 rewires AP-1 for transcriptional reprogramming and lineage plasticity in prostate cancer**. *Nat Commun* 2024, **15**(1):4914. doi:10.1038/s41467-024-49234-9: PMC11162502 The remaining authors declare no competing interests.
13. Qi J, Nakayama K, Cardiff RD, Borowsky AD, Kaul K, Williams R, Krajewski S, Mercola D, Carpenter PM, Bowtell D *et al*: **Siah2-dependent concerted activity of HIF and FoxA2 regulates formation of neuroendocrine phenotype and neuroendocrine prostate tumors**. *Cancer Cell* 2010, **18**(1):23–38. doi:10.1016/j.ccr.2010.05.024: PMC2919332.
14. Han M, Li F, Zhang Y, Dai P, He J, Li Y, Zhu Y, Zheng J, Huang H, Bai F *et al*: **FOXA2 drives lineage plasticity and KIT pathway activation in neuroendocrine prostate cancer**. *Cancer Cell* 2022, **40**(11):1306–1323 e1308. doi:10.1016/j.ccell.2022.10.011:
15. Lu X, Keo V, Cheng I, Xie W, Gritsina G, Wang J, Jin Q, Jin P, Yue F, Sanda MG *et al*: **Epigenetic remodeling and 3D chromatin reorganization governed by NKX2-1 drive neuroendocrine prostate cancer**. *bioRxiv* 2024. doi:10.1101/2024.12.04.626816: PMC11643106.
16. Drost J, Karthaus WR, Gao D, Driehuis E, Sawyers CL, Chen Y, Clevers H: **Organoid culture systems for prostate epithelial and cancer tissue**. *Nat Protoc* 2016, **11**(2):347–358. doi:10.1038/nprot.2016.006: PMC4793718.
17. Park JW, Lee JK, Sheu KM, Wang L, Balanis NG, Nguyen K, Smith BA, Cheng C, Tsai BL, Cheng D *et al*: **Reprogramming normal human epithelial tissues to a common, lethal neuroendocrine cancer lineage**. *Science* 2018, **362**(6410):91–95. doi:10.1126/science.aat5749: PMC6414229.
18. Chen CC, Tran W, Song K, Sugimoto T, Obusan MB, Wang L, Sheu KM, Cheng D, Ta L, Varuzhanyan G *et al*: **Temporal evolution reveals bifurcated lineages in aggressive neuroendocrine small cell prostate cancer trans-differentiation**. *Cancer Cell* 2023, **41**(12):2066–2082 e2069. doi:10.1016/j.ccell.2023.10.009: PMC10878415.
19. Lu X, Keo V, Cheng I, Xie W, Gritsina G, Wang J, Lu L, Shiau CK, He Y, Jin Q *et al*: **NKX2-1 drives neuroendocrine transdifferentiation of prostate cancer via epigenetic and 3D chromatin remodeling**. *Nat Genet* 2025. doi:10.1038/s41588-025-02265-4:

Supplementary Table 1. Antibodies and Primers used in this study

Antibody	Source	Catalog Number	Application
Rabbit recombinant anti-AR	Abcam	Cat#ab108341	WB/IHC
Mouse monoclonal anti-SYP/Synaptophysin	Santa Cruz Biotechnology	Cat#sc-17750	WB/IHC
Rabbit recombinant anti-FOXA2	Abcam	Cat#ab108422	WB/IHC
Rabbit monoclonal anti- PTEN	Cell Signaling Technology	Cat#9188S	WB
Mouse monoclonal anti- p53	Cell Signaling Technology	Cat#2524S	WB
Mouse monoclonal anti-GAPDH	Proteintech	Cat#60004-1-Ig	WB
Mouse monoclonal anti-β-Actin	Santa Cruz Biotechnology	Cat#sc-47778	WB
Rabbit monoclonal anti-Ki67	Abcam	cat#ab16667	IHC

Primers:

Name	Sequence (5′ to 3′)	Application
Ar-F	GAATCCCACATCCTGCTCAA	RT-PCR
Ar-R	GAAAGTCCACGCTCACCATA	RT-PCR
Syp-F	AGTGCCCTCAACATCGAAG	RT-PCR
Syp-R	GCCACGGTGACAAAGAATTC	RT-PCR
Ncam1-F	CCCCACAGGAGTTTAAGGAAG	RT-PCR
Ncam1-R	GTTGGACAGGACTATGAACCG	RT-PCR
Chga-F	AGCATCCAGTTCCCACTTC	RT-PCR
Chga-R	CTCTGTCTTTCCATCTCCATCC	RT-PCR
Insm1-F	AGACAGGTGATCCTCCTTCA	RT-PCR
Insm1-R	GGACACTTTCACCCTGGAAT	RT-PCR

Supplementary Table 2. Upregulated

Gene Symbol	GO term
Bmp4	GOBP_EPITHELIAL_CELL_DIFFERENTIATION
Fstl1	GOBP_EPITHELIAL_CELL_DIFFERENTIATION
Reg3g	GOBP_EPITHELIAL_CELL_DIFFERENTIATION
Cstdc5	GOBP_EPITHELIAL_CELL_DIFFERENTIATION
Lef1	GOBP_EPITHELIAL_CELL_DIFFERENTIATION
Ascl1	GOBP_EPITHELIAL_CELL_DIFFERENTIATION
Six1	GOBP_EPITHELIAL_CELL_DIFFERENTIATION
Insm1	GOBP_EPITHELIAL_CELL_DIFFERENTIATION
Foxa2	GOBP_EPITHELIAL_CELL_DIFFERENTIATION
Cyp1a1	GOBP_EPITHELIAL_CELL_DIFFERENTIATION
Kcnma1	GOBP_EPITHELIAL_CELL_DIFFERENTIATION
Fgfr3	GOBP_EPITHELIAL_CELL_DIFFERENTIATION
Cited1	GOBP_EPITHELIAL_CELL_DIFFERENTIATION
Cdx2	GOBP_EPITHELIAL_CELL_DIFFERENTIATION
Npr2	GOBP_EPITHELIAL_CELL_DIFFERENTIATION
Klf2	GOBP_EPITHELIAL_CELL_DIFFERENTIATION
Spdef	GOBP_EPITHELIAL_CELL_DIFFERENTIATION
Slitrk6	GOBP_EPITHELIAL_CELL_DIFFERENTIATION
Clic5	GOBP_EPITHELIAL_CELL_DIFFERENTIATION
Slc9a4	GOBP_EPITHELIAL_CELL_DIFFERENTIATION
Spink5	GOBP_EPITHELIAL_CELL_DIFFERENTIATION
Krt1	GOBP_EPITHELIAL_CELL_DIFFERENTIATION
Upk1b	GOBP_EPITHELIAL_CELL_DIFFERENTIATION
Slc44a4	GOBP_EPITHELIAL_CELL_DIFFERENTIATION
Tgm1	GOBP_EPITHELIAL_CELL_DIFFERENTIATION
Exph5	GOBP_EPITHELIAL_CELL_DIFFERENTIATION
Krt4	GOBP_EPITHELIAL_CELL_DIFFERENTIATION
Krt75	GOBP_EPITHELIAL_CELL_DIFFERENTIATION
Sprr2h	GOBP_EPITHELIAL_CELL_DIFFERENTIATION
Dnase1l2	GOBP_EPITHELIAL_CELL_DIFFERENTIATION
Vsig1	GOBP_EPITHELIAL_CELL_DIFFERENTIATION
Upk3a	GOBP_EPITHELIAL_CELL_DIFFERENTIATION
Krt15	GOBP_EPITHELIAL_CELL_DIFFERENTIATION
Krt31	GOBP_EPITHELIAL_CELL_DIFFERENTIATION
Bdh2	GOBP_EPITHELIAL_CELL_DIFFERENTIATION

Supplementary Table 2. Downregulated

Gene Symbol	GO term
Sfrp1	GOBP_REGULATION_OF_CELL_DIFFERENTIATION
Col5a1	GOBP_REGULATION_OF_CELL_DIFFERENTIATION
Adamts12	GOBP_REGULATION_OF_CELL_DIFFERENTIATION
Mmp9	GOBP_REGULATION_OF_CELL_DIFFERENTIATION
Serpine2	GOBP_REGULATION_OF_CELL_DIFFERENTIATION
Lgals1	GOBP_REGULATION_OF_CELL_DIFFERENTIATION
Efemp2	GOBP_REGULATION_OF_CELL_DIFFERENTIATION
Smoc1	GOBP_REGULATION_OF_CELL_DIFFERENTIATION
Cela1	GOBP_REGULATION_OF_CELL_DIFFERENTIATION
Tgfb3	GOBP_REGULATION_OF_CELL_DIFFERENTIATION
Adamts9	GOBP_REGULATION_OF_CELL_DIFFERENTIATION
Sema5a	GOBP_REGULATION_OF_CELL_DIFFERENTIATION
Prkd1	GOBP_REGULATION_OF_CELL_DIFFERENTIATION
Dab2	GOBP_REGULATION_OF_CELL_DIFFERENTIATION
Ascl2	GOBP_REGULATION_OF_CELL_DIFFERENTIATION
Egr3	GOBP_REGULATION_OF_CELL_DIFFERENTIATION
Cd34	GOBP_REGULATION_OF_CELL_DIFFERENTIATION
Tgfb1i1	GOBP_REGULATION_OF_CELL_DIFFERENTIATION
Tgfbr3	GOBP_REGULATION_OF_CELL_DIFFERENTIATION
Sema3a	GOBP_REGULATION_OF_CELL_DIFFERENTIATION
Slit1	GOBP_REGULATION_OF_CELL_DIFFERENTIATION
Mef2c	GOBP_REGULATION_OF_CELL_DIFFERENTIATION
Ror2	GOBP_REGULATION_OF_CELL_DIFFERENTIATION
Gli1	GOBP_REGULATION_OF_CELL_DIFFERENTIATION
Lrrk2	GOBP_REGULATION_OF_CELL_DIFFERENTIATION
Ntrk3	GOBP_REGULATION_OF_CELL_DIFFERENTIATION
Vim	GOBP_REGULATION_OF_CELL_DIFFERENTIATION
Foxc1	GOBP_REGULATION_OF_CELL_DIFFERENTIATION
Ntrk2	GOBP_REGULATION_OF_CELL_DIFFERENTIATION
Foxg1	GOBP_REGULATION_OF_CELL_DIFFERENTIATION
Nfatc2	GOBP_REGULATION_OF_CELL_DIFFERENTIATION
Fstl3	GOBP_REGULATION_OF_CELL_DIFFERENTIATION
Lck	GOBP_REGULATION_OF_CELL_DIFFERENTIATION
Sash3	GOBP_REGULATION_OF_CELL_DIFFERENTIATION
Ubash3b	GOBP_REGULATION_OF_CELL_DIFFERENTIATION
Elmo1	GOBP_REGULATION_OF_CELL_DIFFERENTIATION
Fst	GOBP_REGULATION_OF_CELL_DIFFERENTIATION
Ereg	GOBP_REGULATION_OF_CELL_DIFFERENTIATION
Hspa1a	GOBP_REGULATION_OF_CELL_DIFFERENTIATION
Sostdc1	GOBP_REGULATION_OF_CELL_DIFFERENTIATION
Cd109	GOBP_REGULATION_OF_CELL_DIFFERENTIATION
Scube3	GOBP_REGULATION_OF_CELL_DIFFERENTIATION
Vdr	GOBP_REGULATION_OF_CELL_DIFFERENTIATION

Osr1	GOBP_REGULATION_OF_CELL_DIFFERENTIATION
Shox2	GOBP_REGULATION_OF_CELL_DIFFERENTIATION
Alx1	GOBP_REGULATION_OF_CELL_DIFFERENTIATION
Sgk1	GOBP_REGULATION_OF_CELL_DIFFERENTIATION
Myb	GOBP_REGULATION_OF_CELL_DIFFERENTIATION
Prkg2	GOBP_REGULATION_OF_CELL_DIFFERENTIATION
Tiam2	GOBP_REGULATION_OF_CELL_DIFFERENTIATION
Rab7b	GOBP_REGULATION_OF_CELL_DIFFERENTIATION
Meis2	GOBP_REGULATION_OF_CELL_DIFFERENTIATION
Id4	GOBP_REGULATION_OF_CELL_DIFFERENTIATION
Fstl4	GOBP_REGULATION_OF_CELL_DIFFERENTIATION
Inpp4b	GOBP_REGULATION_OF_CELL_DIFFERENTIATION
Ctla2a	GOBP_REGULATION_OF_CELL_DIFFERENTIATION
Elf5	GOBP_REGULATION_OF_CELL_DIFFERENTIATION
Bnc1	GOBP_REGULATION_OF_CELL_DIFFERENTIATION
Ifi204	GOBP_REGULATION_OF_CELL_DIFFERENTIATION
Plekhb1	GOBP_REGULATION_OF_CELL_DIFFERENTIATION